Theoretical investigations of the anisotropic optical properties of distorted 1*T* ReS_2 and $ReSe_2$ monolayers, bilayers, and in the bulk limit

J. P. Echeverry and I. C. Gerber*
LPCNO, Université de Toulouse, INSA-CNRS-UPS, 135 Avenue de Rangueil, 31077 Toulouse, France

(Received 23 November 2017; published 12 February 2018)

We present a theoretical study of electronic and optical properties of the layered ReX_2 compounds (X = S, Se) upon dimensional reduction. The effect on the band-gap character due to interlayer coupling is studied by means of the self-energy corrected GW method for optimized and experimental sets of a structure's data. Induced changes on the optical properties as well as optical anisotropy are studied through optical spectra as obtained by solving the Bethe-Salpeter equation. At the G_0W_0 level of theory, when decreasing the thickness of the ReS_2 sample from bulk to bilayer and to a freestanding monolayer, the band gap remains direct, despite a change of the band-gap nature, with values increasing from 1.6, 2.0, and 2.4 eV, respectively. For $ReSe_2$, the fundamental band gap changes from direct for the bulk phase (1.38 eV) to indirect in the bilayer (1.73 eV) and becomes direct again for a single layer (2.05 eV). We discuss these results in terms of the renormalization of the band structure. We produce the polarization angular-dependent optical response to explore the optical anisotropy present in our results, as well as the fine structure of the lowest excitonic peaks present in the absorption spectra.

DOI: 10.1103/PhysRevB.97.075123

I. INTRODUCTION

Isolation of a single and few layers from the bulk's systems in many transition-metal dichalcogenides (TMDCs) has renewed interest in their structural and optical properties broadly studied in bulk [1–6]. Dimensionality reduction effects have motivated recent works on monolayers (MLs) and few-layers-thick systems since it has been shown for the first time in MoS_2 that upon dimensional confinement, the indirect band gap in bulk becomes direct in a ML [7,8]. Today, several others systems such as W-based systems have shown similar behavior [9–11].

Such is the case for ReX_2 (X = S, Se) compounds, i.e., layered crystals belonging to the TMDC semiconductor family which crystallize in a distorted 1*T* diamond-chain structure with triclinic symmetry unit cell, usually denoted 1*T*′. The successful isolation of a single and few layers of ReX_2 has allowed their structural and optical characterization [12–15]. However, there are many aspects of ReX_2 optoelectronic properties that still remain to be clarified. See Ref. [16] for a recent review of experimental aspects of these TMDCs.

Based on their findings, some groups have argued that in ReS_2, the interlayer coupling is negligible and the stacked layers in bulk behave as electronically and vibronically decoupled monolayers [12,17]. In contrast, recent photoluminescence (PL) and reflectance spectroscopy measures in bulk and few-layer-thick samples of ReS_2 reveal a dependence of the optical properties on the thickness [15]. Additionally, it was usually claimed that ReS_2 shows a transition from indirect to direct optical band gap when the dimensionality is reduced from bulk to ML, as in many other TMDCs [18]. This is in contradiction to the work of Tongay *et al.* who have reported an unchanged indirect band gap from bulk to ML. A very recent work on ReS_2 bulk, using gated field-effect transistors, tends to confirm the indirect character of the gap [19], while recent angle-resolved photoemission spectroscopy (ARPES) experiments tend to prove the contrary [20].

From the theoretical side, some attempts to clarify these subjects using different methodologies can be found in the literature. Early results on the bulk's band structures based on density functional theory (DFT) have shown ReX_2 compounds to be indirect band-gap semiconductors [21], while more recent theoretical studies tend to prove the contrary [12]. For ML and few-layer systems at the standard DFT level, i.e., in which many-body screening effects are scarcely described, the fundamental gap is found to be direct but largely underestimated for ReS_2 [12,22–24]. On the contrary, a $ReSe_2$ ML has an indirect band gap when explicit electron-electron screening is taken into account [14,22]. The only attempts to describe the ReX_2 ML with the use of the GW self-energy correction also give a direct gap of 2.38 eV at the Γ point, i.e., at the center of the first Brillouin zone (BZ), for ReS_2 as for $ReSe_2$ ML [22,25]. However, for the latter case, nothing is said about the difference between the indirect and the direct transition since it is known that for different computational settings and/or a small strain effect, it is easy to influence the position of valence-band maxima and conduction-band minima [26].

The presence of a strong optical anisotropy in ReX_2 compounds [27–30], unlike Mo- or W-based hexagonal TMDCs, is due to their particular crystalline structure (see Fig. 1). It is believed that the structural distortion leads to a much weaker interlayer coupling, so the band renormalization is supposedly absent and bulk ReX_2 should behave as decoupled monolayers [12,13]. However, Aslan *et al.* [15] demonstrated that the anisotropic optical properties of single- and few-layer ReS_2 crystals are different through polarization-resolved reflectance and photoluminescence spectroscopy. They have found that

*igerber@insa-toulouse.fr

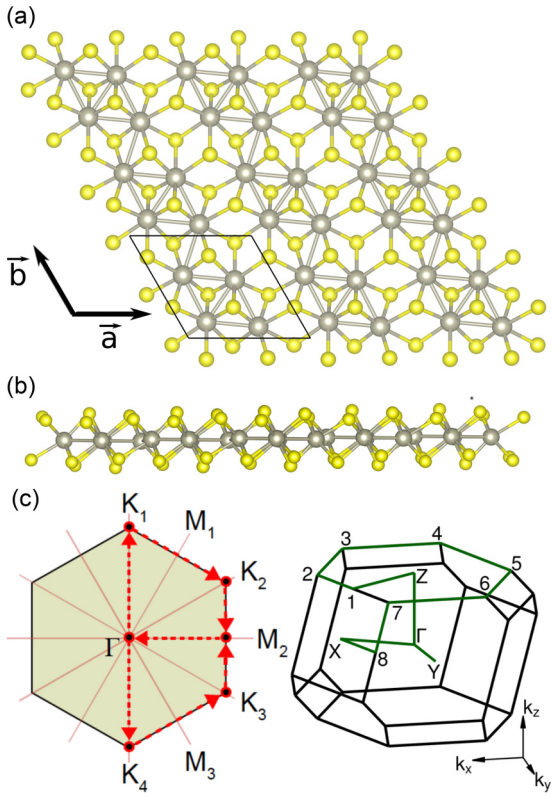

FIG. 1. (a) Top view and (b) side view of distorted 1T monolayer ReX_2; Re atoms are in gray and X (S, Se) atoms are in yellow. The cell used during calculations is depicted by a black line in (a). The Re chain is along the $\vec{b}$ direction. (c) First Brillouin zone of the ReX_2 monolayer and bulk. For the sake of comparison, the notation is the same as the one used in Ref. [25].

the near band-edge excitons in ultrathin crystals absorb and emit light with preferred linear polarizations. Likewise, they have observed that the transition energies of the excitons can be tuned with layer thickness. They have thus established that ultrathin ReS_2 has optical transitions with strengths and transition energies that depend on the thickness and polarization of the optical radiation.

Here we propose to explore theoretically the optical properties of a freestanding ML and a bilayer (BL) of ReX_2 systems by including excitonic effects through GW and Bethe-Salpeter equation (BSE)-type calculations and compare them to the bulk's spectra. We address the question about the character of the fundamental band gap upon dimensional reduction and we discuss it in terms of screening effects due to the presence of neighboring layers. Likewise, we discuss the dependence of the optical spectra on the thickness and on the polarization angle by rotating the dielectric tensor's components on the layer's plane. The present paper is organized as follows: in Sec. II, we present the computational details for ML, BL, and bulk calculations. In Sec. III, the results concerning the quasiparticle band structure of ML, BL, and bulk, as well as the effects on the nature of the transition band gaps when increasing the thickness, are presented. Optical adsorption spectra for ML, BL, and bulk are discussed in Sec. IV. Finally, we present the main conclusions of this work in Sec. V.

II. COMPUTATIONAL DETAILS AND ATOMIC STRUCTURES

The atomic structures, the quasiparticle band structures, and optical spectra are obtained from DFT calculations using the VASP package [31,32]. The Perdew-Burke-Ernzerhof (PBE) functional [33] is used as an approximation of the exchange-correlation electronic term. Core electrons are treated by the projector augmented wave scheme [34,35]. Fifteen electrons for Re atoms and six for S, Se atoms are explicitly included in the valence states. All atoms are allowed to relax with a force convergence criterion below 0.005 eV/Å. During bulk and BL geometry optimization calculations, the functional of Langreth and Lundqvist [36,37] is used in the van der Waals (vdW)-DF2 form [38,39] in order to accurately describe long-range correlations between layers. A grid of $6 \times 6 \times 1$ k points has been used, in conjunction with a vacuum height of around 20 Å, to benefit from the error cancellation in the band-gap estimates [40] and to provide the imaginary part of the dielectric constant, which is a key quantity in absorption spectra in reasonable agreement with experiments as suggested in different works [41,42] for ML and BL calculations. A grid of $6 \times 6 \times 6$ k points has been used for the bulk calculations. As can be seen in Appendix A, using a $6 \times 6 \times 1$ grid ensures a variation of only 50 meV compared to a $12 \times 12 \times 1$ calculation for the position of the first excitonic peak. We use an energy cutoff of 400 eV and a Gaussian smearing with a width of 0.05 eV for partial occupancies, when a tight electronic minimization tolerance of 10^{-8} eV is set to determine with a good precision the corresponding derivative of the orbitals with respect to k needed in quasiparticle band structure calculations. Spin-orbit coupling was also included non-self-consistently to determine the eigenvalues and wave functions as input for the full-frequency-dependent GW calculations [43] performed at the G_0W_0 level, but also at the GW_0 level with two iterations of the G term for testing purposes. The total number of states included in the GW procedure is set to 600, in conjunction with an energy cutoff of 100 eV for the response function, after a careful check of the direct band-gap convergence, to be smaller than 0.1 eV in the function of k-point sampling too. Band structures have been obtained after a Wannier interpolation procedure performed by the WANNIER90 program [44]. Only direct optical excitonic transitions are calculated by solving the BSE [45,46], with the inclusion of six valence and eight conduction bands in the diagonalization process for ML and bulk calculations. For the BL systems, we use 12 valence and 16 conduction bands; for all optical spectra, a broadening parameter of 25 meV is set. From these calculations, we report the absorbance values defined as proposed in Ref. [47], by using the imaginary part of the complex dielectric function $\epsilon_2(\omega)$, with the following formula:

$$A(\omega) = \frac{\omega}{c}\epsilon_2(\omega)\Delta z, \tag{1}$$

where Δz is the vacuum distance between periodic images of the ML and BL. This quantity is measurable and supposedly should not depend on the size of the calculation cells in the ML/BL perpendicular direction. As pointed out by Bernardi *et al.* [48], Eq. (1) is a Taylor expansion for $\Delta z \to 0$ of the absorbance defined as $A = 1 - e^{-\alpha_2 \Delta z}$ for a single or bilayer of

TABLE I. Calculated and experimental lattice parameters and angles for bulk and monolayer ReX_2 systems.

	a (Å)	b (Å)	c (Å)	α (°)	β (°)	γ (°)
ReS_2						
Expt. bulk[a]	6.510	6.417	6.461	106.47	88.38	121.10
DFT bulk	6.57	6.42	6.34	104.2	93.7	119.8
ML D_1	6.57	6.40				119.8
ML D_2	6.50	6.40				118.7
$ReSe_2$						
Expt. bulk[b]	6.716	6.602	6.728	104.90	91.82	118.94
DFT bulk	6.86	6.68	6.76	103.8	95.0	119.8
ML D_1	6.84	6.65				119.7

[a]Reference [51].
[b]Reference [52].

a bulk material with a thickness Δz, presenting an absorption coefficient $\alpha_2(\omega) = \frac{\omega\epsilon_2(\omega)}{cn(\omega)}$, where for this case the refractive index is $n = 1$ since the considered ML/BL is surrounded by vacuum only.

Considering the lattice parameters and atomic positions in the bulk, as well as in ML or BL stacking, few issues need to be addressed. In the bulk's case, as can be seen in Table I , the lattice parameters and the angles obtained upon geometry optimization using a van der Waals correction are in good agreement with the experimental data for both materials. We recall that the $1T'$ structure observed experimentally for bulk ReX_2 phases and used here for atomic configurations is triclinic, the corresponding space group being $P\bar{1}$. As a consequence, MLs and bulk present a center of inversion, and the symmetry point group is thus C_i. For the ML systems, PBE optimization results (denoted D_1) are in line with previous theoretical studies [14,22,49]. Additionally we also report the D_2 structure as proposed in Ref. [50], which corresponds to a diamond flip or a displacement of Re atoms along the lattice vector b, with a small strain. Interestingly, it implies a slight decrease of around 1% of the a parameter. Since the work of Tongay *et al.* [12], it is believed that contrary to other TMDCs, ReX_2 systems possess very weak interlayer interactions. However, when nonlocal correlations are properly taken into account, it appears that the binding energy between two layers in the simplest AA stacking (a simple superposition of the two layers) is roughly the same as in the emblematic MoS_2 case; see Appendix B.

In order to investigate the BL stacking, we have kept fixed the lattice parameters from ML D_1 structures and displaced the upper layer in different directions, along $\vec{a}$, along $\vec{b}$, and perpendicular to $\vec{b}$, as proposed in previous studies [12,49]. We have taken into account the effects of van der Waals forces in the exchange-correlation term, contrary to previous works, and thus the resulting optimized stacking order is slightly different. For both ReS_2 and $ReSe_2$ systems, the most stable stacking is yielded when the second layer is displaced by 0.375 $\vec{a}$ from the AA stacking, losing the presence of a center of inversion in the calculation's cell. Note that the energy landscape is very flat with minima only separated by energy differences around a few tenths of meV, as shown in Appendix C.

III. BAND STRUCTURES AND QUASIPARTICLE BAND GAPS

A. Monolayer

The G_0W_0 band structures of distorted $1T$-ReS_2 ML in D_1 and D_2 phases are plotted in Fig. 2 along high-symmetry directions of the first BZ. A relatively flat dispersion of the bands near Fermi energy is observed, due to the strongly localized characters of the involved orbitals of the Re atoms. Indeed, the main orbital contributions, estimated by a crude decomposition of the electronic states on atomic spherical harmonics, to the highest valence band (HVB) in Γ come from all five 5-d Re orbitals, with a very modest mixing with the $3p$ S orbitals, mainly the p_z ones. We recall that in the C_i symmetry point group, the d orbitals are of even parity. For the lowest conduction bands (LCBs), the electronic states are mainly distributed on the Re d_{xy} and d_{z^2} orbitals, with a much stronger mixing with p_x and p_y orbitals of sulfur atoms. This hybridization is thus responsible for the change of parity required to allow the transition. Comparing with others TMDCs such as Mo or WX_2, ReX_2 does not present spin splitting due to spin-orbit coupling (SOC) in the ML limit since inversion symmetry is present. This has visible effects on its optoelectronic properties as discussed below. Thus HVB and LCB are spin folded with a negligible splitting between them. Interestingly, the band structures of both D_1 and D_2 phases are very similar, with only slight changes of the band curvatures in the K_1, K_4 valleys for both HVB and LCB. From this result, we can extract a value of the fundamental gap located in the center of the first BZ, E_g^{Γ}, for ReS_2 ML to be 2.38 eV, in remarkably good agreement with the previous work of Zhong *et al.* [22]. Note that when reducing lattice parameters to the experimental values, the ReS_2 ML remains direct with a slightly smaller gap, 2.23 eV.

The $ReSe_2$ ML's band structure, with D_1 DFT-optimized lattice parameters, is shown in Fig. 2 (right side). Flat bands near the Fermi level are also obtained, making the $ReSe_2$ ML band structure very similar to ReS_2. The fundamental gap remains direct with a value of 2.05 eV. This result is in line with the reported value of 2.09 eV in Ref. [22], but much smaller than the 2.44 eV proposed in the work of Arora *et al.* [25]. For the sake of comparison, we report in Fig. 2 the behavior of the HVB and LCB around the Γ point for the D_1 DFT-optimized lattice parameters and the experimental ones, taken as in the bulk phase. Interestingly, when decreasing the lattice parameters, the $ReSe_2$ fundamental gap becomes indirect since a maximum [denoted Λ in the HVB along the Γ-K_1 (-K_4) direction] pops up, and the direct gap remains 10 meV larger. This observation has already been reported in a previous study of ReX_2, but without any explanation [22]. The importance of lattice parameter choices has been pointed out in a previous work on MoX_2 ML systems [26], especially when Se atoms are involved. As usual, the use of partially self-consistent G_2W_0 calculations provides larger band-gap values, without changing the positions of the VB maxima and CB minima. The direct gap in Γ values is 2.60 and 2.23 eV for ReS_2 and $ReSe_2$, respectively, at this level of theory.

B. Bilayer

Figure 3 provides band structures for both ReS_2 and $ReSe_2$ BLs. In both cases, no spin splitting is observed. The interlayer

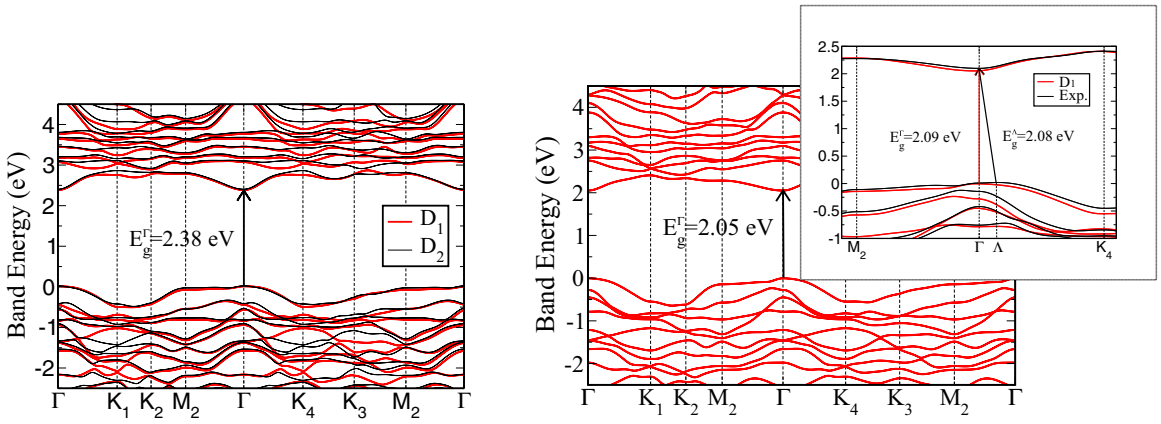

FIG. 2. Left: The G_0W_0 band structures of the ReS_2 monolayer in the D_1 (red) and D_2 (black) phases. Right: The G_0W_0 band structures of the $ReSe_2$ monolayer in the D_1 phase. The inset presents a zoom around the Γ point for two sets of lattice parameters: the DFT-optimized lattice parameters of the D_1 phase and the experimental ones. The energy level of the valence-band maximum (in Γ) is set to zero.

coupling impacts the band structure by renormalizing the band gap by roughly 16%. For ReS_2 BL, the positions of the CB minimum and the VB maximum remain the same as in the ML case. As a consequence, the ReS_2 BL band gap is still direct in Γ and is decreased to 2.00 eV. This is clearly different for the MoX_2 or WX_2 families, for which drastic changes in the LCB are observed [53]. This observation tends to confirm the existing electronic decoupling between ReS_2 layers evidenced in experimental works [12,17]. However, for the $ReSe_2$ BL, it is less obvious. On the one hand, similarly to the ML case, the VB maximum is slightly shifted from the Γ point along the Γ-K_1 (-K_4) direction; on the other hand, the CB minimum is also slightly shifted away from Γ in the Γ-M_2 direction. Thus, E_g is indirect with a value of 1.73 eV, when the direct gap in Γ is 1.77 eV. We have checked that the influence of the stacking order on the band-gap value is very limited since, for ReS_2 BL in an AA-stacking configuration, E_g^Γ is 2.04 eV.

C. Bulk

In Fig. 4 is plotted the self-energy corrected ReS_2 bulk's band structure using high-symmetry directions, as in Fig. 1. Our G_0W_0 calculation predicts bulk ReS_2 to be a semiconductor with a direct fundamental band gap of 1.60 eV in Z (0,0,1/2) coordinates, while the in-plane dispersion does not change that much with a HVB-LCB separation of 1.88 eV at the Γ point. Those values are in the same range as the ones reported recently in Ref. [25]. This is clearly different from other Mo- and W-based MX_2 families, where the HVB maxima always remain at Γ and, at the same time, the LCB minima still lie in the (k_x,k_y) plane. For those systems, relatively strong interactions between the chalcogen atoms of the neighboring layers result in the direct-to-indirect band-gap crossover with increasing the number of layers, while for Re systems, the nature of the band gap itself is changed, favoring interlayer transitions. Indeed, a closer look at the orbital's character of those states clearly proves a very pronounced d_{z^2} character. The one-shot GW band structure of bulk $ReSe_2$ is given in Fig. 4. We observe a direct fundamental band gap of 1.38 eV at the Z symmetry point. In the (k_x,k_y) plane, the top of the HVB is still located between Γ and K_4 (K_1) and the bottom of the LCB remains in the vicinity of the K_3 symmetry point, mainly retaining the in-plane band structure of the BL case.

A significant band dispersion of the bands near the Fermi level is observed in the bulk's band structure compared with the ML and BL cases for both ReS_2 and $ReSe_2$. It is mainly due to interlayer interaction. Likewise, one can note a blueshift

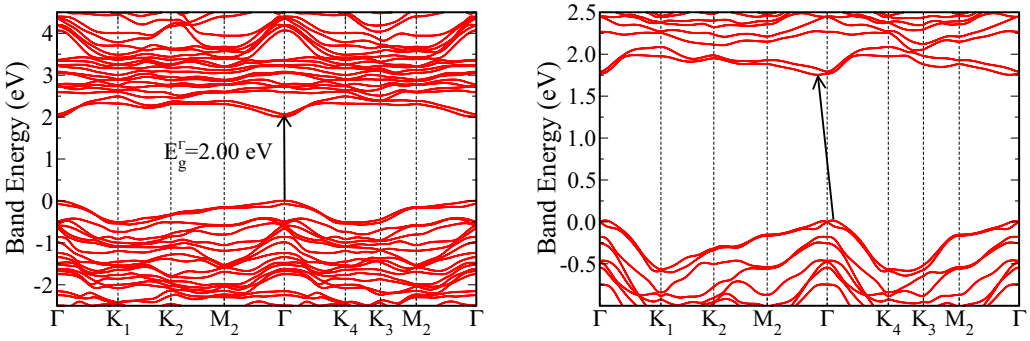

FIG. 3. Left: The G_0W_0 band structures of ReS_2 bilayer in the most stable configuration, i.e., with a displacement of around 2.4 Å along the $\vec{a}$ of the second layer. Right: The G_0W_0 band structures of $ReSe_2$ bilayer in the most stable configuration, i.e., with a displacement of around 2.4 Å along the $\vec{a}$ of the second layer. The energy level of the valence-band maximum (in Γ) is set to zero.

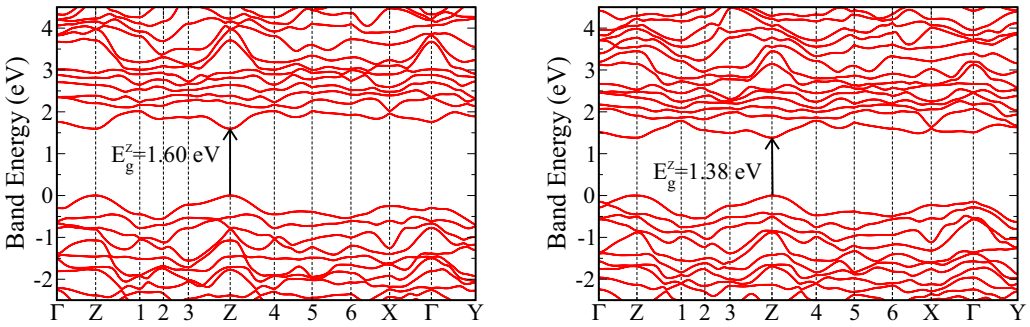

FIG. 4. The G_0W_0 band structures of ReS_2 bulk (left) and $ReSe_2$ bulk (right). The energy level of the valence-band maximum (in Z) is set to zero. High-symmetry directions of the 1BZ in bulk crystal are depicted in Fig. 1.

of the band-gap value upon dimensional reduction from bulk to ML as expected.

IV. ABSORBANCE

The absorbance of a single ReS_2 ML, in the D_1 structure, as a function of the frequency for the xx (Γ-M_2 direction) and yy (Γ-K_1 direction) components, is given in Fig. 5. We recall that in ML cases for both ReX_2 systems, the valence-band maxima (VBM) and conduction-band minima (CBM) are doubly degenerated. This implies, as proposed by Arora *et al.* [25], that the first four peaks' origins are the four interband transitions with different combinations of spin. As a consequence, they are split due to exchange interaction. This is clearly shown in the inset of the left part of Fig. 5. As soon as the active space of the BSE calculations includes at least two occupied and two virtual states, the exchange term splits excitons in two different directions. Optical anisotropy is clearly evidenced in the spectrum. The main excitonic features appear in the energy range between 1.5 and 2.4 eV. While the most stable exciton, at 1.64 eV, has contributions along the xx and yy directions, the second one, which lies 0.05 eV higher in energy, is mainly oriented along the Γ-M_2 (xx) direction. A similar behavior is observed for $ReSe_2$ ML with smaller intensities and a less pronounced anisotropic character in the first two excitonic peaks. We stress the fact that in other TMDCs, this splitting does not involve anisotropy, but exchange interaction and SOC [54]. Interestingly, in Ref. [15], they report an optical gap value of 1.61 eV for ReS_2 ML using PL and reflectance spectroscopy experiments. For $ReSe_2$ ML, the experimental optical gap is 1.50 eV [25], while it is located at 1.43 eV in our calculations. The overall agreement between experimental results and our estimates is good, considering the precision of the GW+BSE calculations scheme.

The binding energy (BE) of the lowest exciton in ReS_2 ML is 0.74 eV, much larger than other M- or W-based TMDCs. For $ReSe_2$ ML, the BE is 0.57 eV when the exchange splitting is only 0.04 eV. The binding-energy values are in line with previous reports; they only differ due to different computational details [22,25]. Additionally, we have noticed the fine structure of those peaks with the presence of a dark state that is 7 meV lower in energy than the bright one, and the presence of a gray exciton, possibly coupled to light with z polarization as recently observed in WSe_2 ML [55], with a small oscillator strength 4 meV above the bright state. The next-higher-energy peak is seen at 1.83 eV with a stronger oscillator strength for the yy component than for the xx one.

When a second layer is added to a ReS_2 ML, with two different stacking orders, there is a redshift of the lowest excitonic peak of 0.04 eV. One can still observe the anisotropic character by decomposing the absorbance function in the xx and yy directions. The orientation of the second layer with

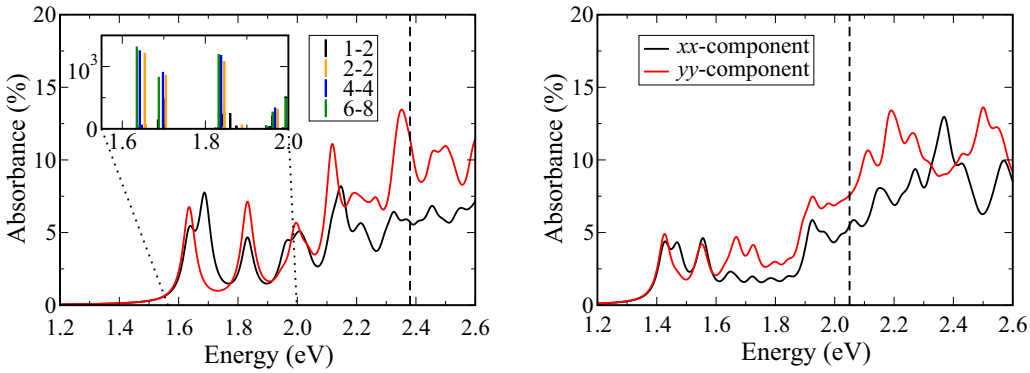

FIG. 5. Absorbance of monolayer ReS_2 (left) and $ReSe_2$ (right) in the Γ-M_2 direction (xx) and Γ-K_1 direction (yy). The vertical dashed line represents the fundamental band-gap energy. The inset of the left figure presents the oscillator strengths with respect to the number of occupied and unoccupied states included in the BSE calculations.

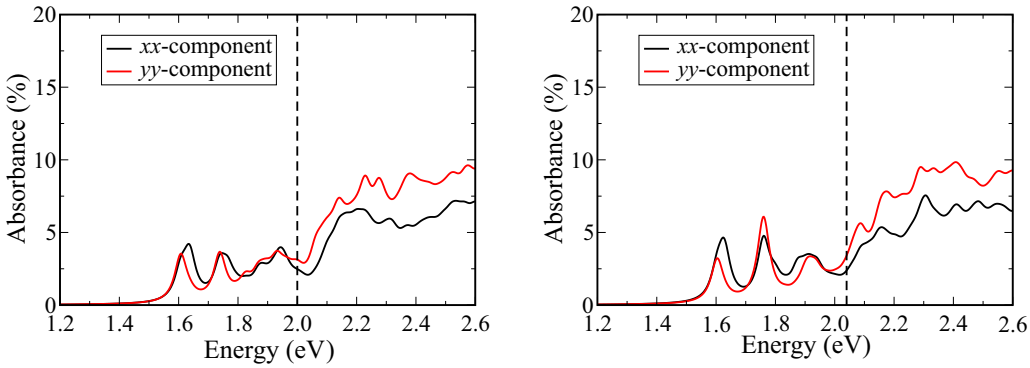

FIG. 6. Absorbance of ReS_2 BL in the optimized configuration (left) and in the AA-stacking configuration (right) in the Γ-M_2 direction (xx) and Γ-K_1 direction (yy). The vertical dashed line represents the fundamental band-gap energy.

respect to the first one does not drastically change the spectrum. The only noticeable difference can be seen when the stacking is highly symmetric (AA stacking) (see Fig. 6), where the peak at 1.76 eV is much more intense due to the perfect alignment between the atomic positions. The corresponding BE is 0.40 eV for the optimized stacking order and slightly larger (0.44 eV) for AA stacking. The screening effect on the first ReS_2 ML due to the presence of a second layer does not have a significant effect on the energy of the electronic transitions, while the band-gap renormalization induces important changes to the BE. Despite the fact that a $ReSe_2$ BL has an indirect band gap in our calculations, we have performed BSE calculations in order to investigate direct transitions. As for ReS_2 BL, those direct-transition energies are not altered by the addition of a second layer in $ReSe_2$. The first two direct transitions are still located at 1.41 and 1.44 eV for the BL, and a similar trend is obtained for ReS_2. Thus the electronic screening due to the second layer in ReX_2 compounds only implies a reduction of the fundamental gap, possibly altering its direct-to-indirect character for $ReSe_2$ only and significantly reducing the BE.

Figure 7 shows the absorption coefficient α_2 as a function of the frequency for both bulks of the ReS_2 and $ReSe_2$ systems. Both spectra present a rich excitonic structure in the energy range from 1.3 to 1.6 eV. By comparing in-plane contributions to the dielectric tensor, we clearly evidence the optical anisotropy still present in the bulk phase of Re-based TMDCs. In the mentioned energy range, we observe that the excitonic response is slightly stronger for the yy component than for the xx one. For ReS_2, the lowest-lying feature appears now at 1.40 eV, in good agreement with the experimental determination of the optical gap of Ref. [15], i.e., 1.47 eV. Reference [15] also reports the presence of a feature at 1.4 eV in PL but not in reflectance experiments. Based on this, they have concluded that bulk ReS_2 is a semiconductor with indirect excitonic band gap. Marzik *et al.* [56] have determined from their photoelectrochemical measurements an indirect band gap of 1.4 eV for ReS_2 single crystals, while from low-temperature absorption measurements, Friemelt *et al.* [28] have determined a value of 1.56 eV for the direct optical band gap of p-type ReS_2 single crystals and 1.53 eV for n-type ones. Furthermore, they have also found a sharp peak in the low-temperature absorption spectrum at 1.57 eV, which was assigned to an excitonic peak. These values are in reasonable agreement with our findings, but the assignment contrasts with our conclusion since our band structure results confirm a direct fundamental gap for ReS_2 in bulk, in the Z k point. Concerning the optical band gap, we safely assign the feature present at 1.40 eV to be a direct excitonic band gap since in any BSE calculation only vertical transitions are taken into account. Two others intense peaks at 1.51 and 1.56 eV are theoretically determined, in very good agreement with values extracted from reflectance

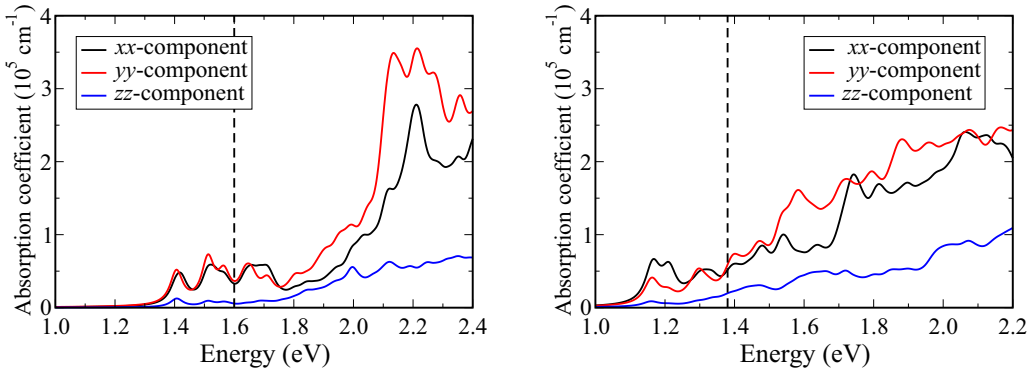

FIG. 7. Optical absorption coefficient of bulk ReS_2 (left) and $ReSe_2$ (right) in the Γ-M_2 (xx), Γ-K_1 (yy), and Γ-Z (zz) directions. The vertical dashed line represents the fundamental band-gap energy.

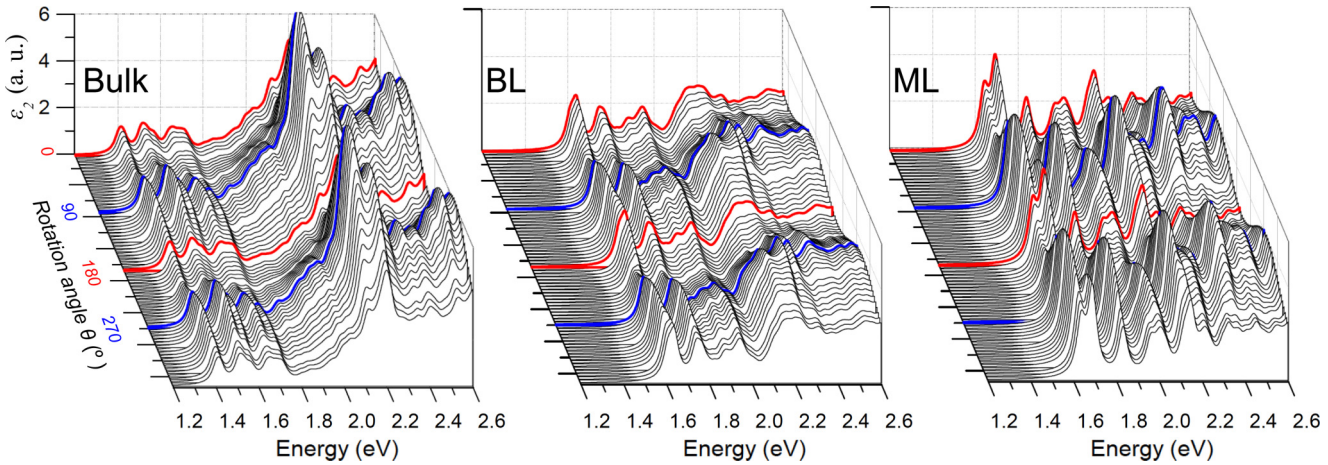

FIG. 8. Imaginary part of the dielectric tensor of ReS_2 systems, with respect to the light polarization angle.

contrast measurements, 1.51 and 1.58 eV. The theoretical blueshift when decreasing the thickness of the sample is thus 0.24 eV, while its experimental value is 0.14 eV [15]. The next two main features are shifted in energy by 0.18 and 0.27 eV, respectively, while experimentally those values are 0.16 and 0.30 eV. The BE of exciton in ReS_2 bulk is thus estimated to be 0.20 eV, reduced by 75% when compared to the ML limit.

For $ReSe_2$ in the bulk phase, the lowest-energy peak in the spectra is composed of three bright excitons; the dominant strength oscillator exciton is located at 1.16 eV and it is preceded by a couple of weaker strength oscillator excitons located a few meV lower. The BE of bulk $ReSe_2$ is 0.22 eV considering the direct fundamental band gap also located in Z. Previous experimental works [52,56,57] using different techniques have obtained values of 1.15, 1.17, and 1.22 eV, respectively, for a single-crystal optical band gap. More recently, PL experiments [58] report a value of 1.26 eV for the optical band gap of bulk $ReSe_2$, when a larger value (1.37 eV) is also proposed [25]. Globally in this case, the dispersion of the optical band gap is still relatively large. The next-higher-energy features are centered around 1.21 and 1.29 eV, with the latter being broader for the xx component. As a consequence, the blueshift observed on the first two peaks when reducing layer thickness from bulk to ML is 0.27 and 0.26 eV, respectively. This is clearly much larger than in any other TMDCs, but is probably overestimated in our calculations, when compared to experiments [25]. The corresponding excitonic BE is 0.21 eV.

In order to study the optical anisotropy of ReX_2 compounds and, in particular, to understand the angular dependence of the low-energy features in the spectra, we have rotated the in-plane dielectric tensor component on the layer around the $\vec{c}$ axis (perpendicular to $\vec{a}$ and $\vec{b}$). In Fig. 8, the imaginary part of the dielectric tensor of ReS_2 systems as a function of the polarization angle and the energy of the incoming light is presented. $ReSe_2$ results are given in Appendix D. The blue line corresponds to the yy dielectric tensor component. We note that the optical anisotropy near the excitonic resonances implies that the absorption of these layers varies strongly as a function of the light polarization. For the low-lying features below the fundamental gap values, the maximum is always obtained for light polarization aligned with the Re-Re chain, so with an angle of around 120°, for ML, BL, and bulk too.

From bulk to ML thickness, one can see an increase of the lowest excitonic peak's intensities as well as a blueshift of their transition energies. For each excitonic feature in the spectra, one can identify the easy polarization axis, a preferential direction where transition probability becomes maximum. The angle where the intensity reaches a minimum corresponds to the weakest oscillator strength or a polarization angle where transitions are forbidden. We note that the oscillator strength of the excitons in the lowest features of ML and BL has a different easy polarization direction. As a consequence, in the angular evolution of the features, those excitons seems out of phase. The variation of the intensity of the lowest-energy features from the xx component to the yy component is evidence of the optical anisotropy of the ReX_2 compounds. The oscillator strength of the excitonic features becomes stronger over dimensional reduction.

V. CONCLUSION

In the present work, we propose a theoretical study of electronic and optical properties of the layered ReX_2 compounds for the ML, BL, and bulk phase, by means of the GW+BSE scheme. For ReS_2, the band gap remains direct, despite a change of the band-gap nature, with values increasing from 1.6, 2.0, and 2.4 eV from bulk to ML, respectively. For $ReSe_2$, the fundamental band gap changes from direct for the bulk phase (1.38 eV) to indirect in the bilayer (1.73 eV), and becomes direct again for a single layer (2.05 eV). Those results are compatible with experimental findings, and theoretical absorption spectra agree well with results from PL and reflectance experiments. Anisotropic optical properties are also evidenced and the fine structure of the excitons certainly deserve further experimental work.

ACKNOWLEDGMENTS

J.P.E. thanks the ANR-14-CE26-0017 project for financial support. The authors also acknowledge the CALMIP initiative for the generous allocation of computational time, through Project No. p0812, as well as the GENCI-CINES, GENCI-IDRIS, and GENCI-CCRT for Grants No. x2016096649 and No. A0020906649.

APPENDIX A: CONVERGENCE ISSUE OF THE IMAGINARY PART OF THE DIELECTRIC CONSTANT WITH RESPECT TO *k*-POINT SAMPLING

To investigate convergence issues with respect to the *k*-point sampling, we have neglected the SOC term but kept all the others calculation parameters as they are given in Sec. II. If one checks the first excitonic peak in the imaginary part of the dielectric constant, as shown in Fig. 9, for three different grids, the difference is around 0.05 eV. The position of higher-energy excitons also follows the same trend, but with a $12 \times 12 \times 1$ grid, new features appear, probably due to a better description of the excited states of the excitons. Note that by adding the SOC term, symmetry is removed in the calculation, thus significantly increasing the computational cost, which makes a $12 \times 12 \times 1$ calculation intractable in a reasonable time.

APPENDIX B: BINDING ENERGY OF MoS_2 AND ReS_2 BILAYERS

In Fig. 10, the binding energy of MoS_2 and ReS_2 bilayers in AA stacking is given. PBE results are compared to the curves obtained by the Tkatchenko-Scheffler method [59], the DFT-D3 method [60], or the vdW-DF2 scheme [38,39]. A globally similar range of energy is obtained, meaning that ReS_2 behaves like all the other TMDCs in terms of van der Waals interactions between layers.

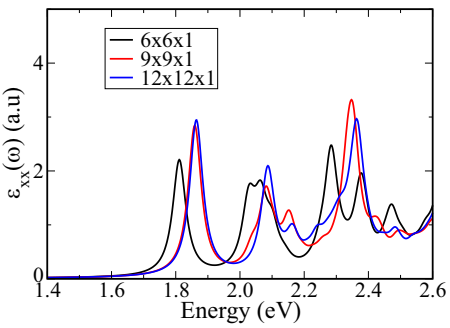

FIG. 9. Imaginary part of the dielectric tensor of ReS_2 ML dependent on *k*-point sampling grids.

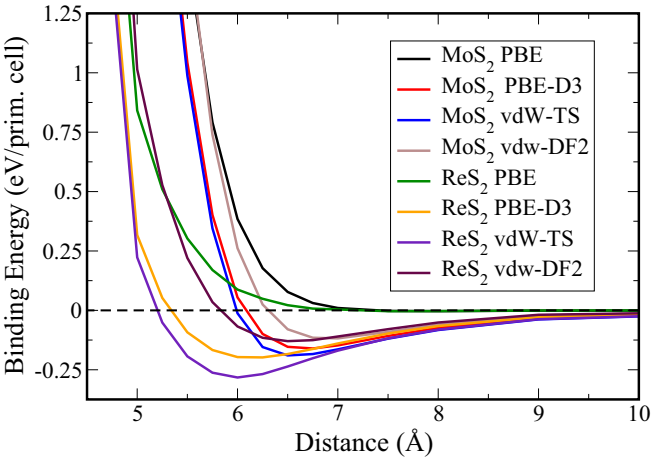

FIG. 10. Comparison between the binding energy of MoS_2 and ReS_2 BL for different schemes that include van der Waals forces in the hypothetical AA stacking.

APPENDIX C: STACKING GEOMETRIES OF ReS_2 BILAYERS

The stability of the stacking with respect to translational displacement, along $\vec{a}$, and along as well as perpendicular to $\vec{b}$, has been investigated using the vdW-DF2 functional. In Fig. 11, the primitive cell and the lattice vectors' directions are recalled, as well as the energy differences from the hypothetical AA stacking, i.e., the simplest superposition of the two layers. Also, the atomic positions were allowed to relax.

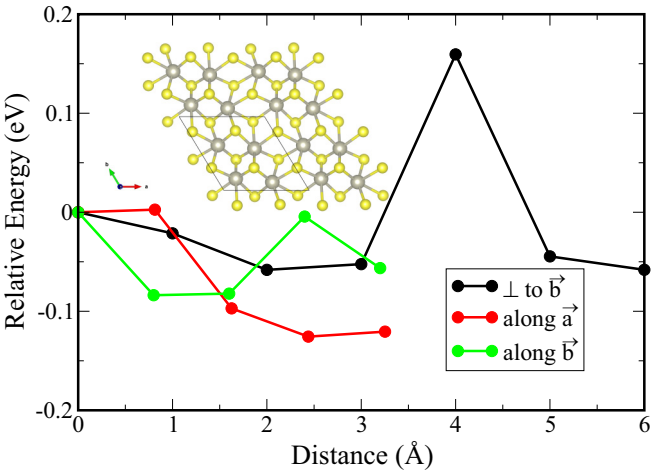

FIG. 11. Energy differences from AA stacking for various distances in three directions of displacement.

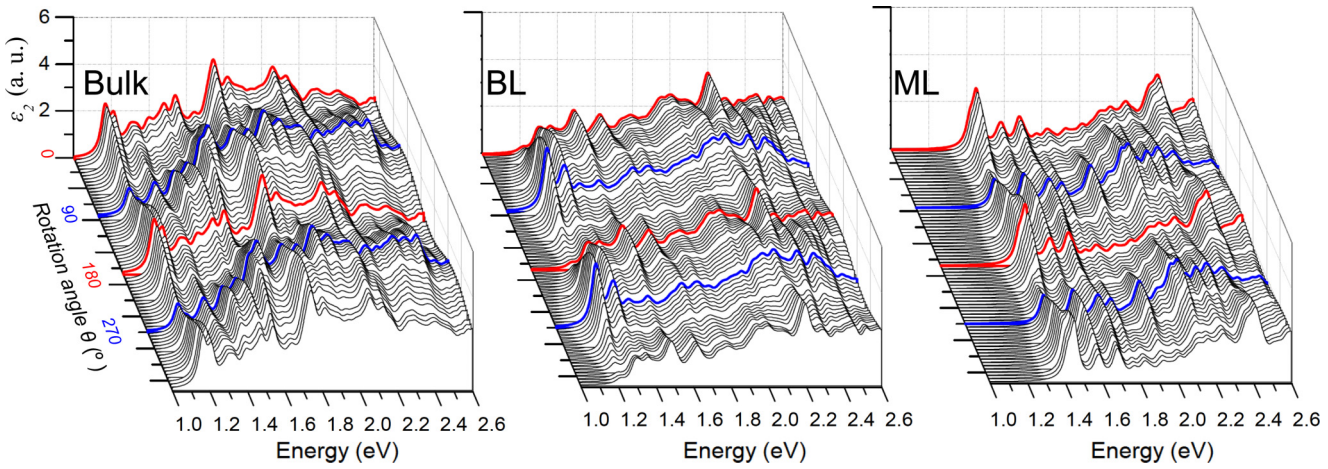

FIG. 12. Optical absorption spectra of $ReSe_2$ systems, with respect to the light polarization angle.

APPENDIX D: POLARIZATION ANGULAR DEPENDENCE OF THE ABSORPTION SPECTRA FOR $ReSe_2$ SYSTEMS

Figure 12 presents the optical absorption spectra of $ReSe_2$ systems, with respect to the light polarization angle. As for ReS_2 system one can note that the optical anisotropy is clearly evidenced. The absorbance varies strongly as a function of the light polarization. Maxima of the first excitonic peaks correspond to light polarization aligned with the Re-Re chain.

[1] C. H. Ho, P. C. Liao, Y. S. Huang, T. R. Yang, and K. K. Tiong, J. Appl. Phys. **81**, 6380 (1997).
[2] C. H. Ho, P. C. Liao, Y. S. Huang, and K. K. Tiong, Phys. Rev. B **55**, 15608 (1997).
[3] C. H. Ho, Y. S. Huang, K. K. Tiong, and P. C. Liao, J. Phys.: Condens. Matter **11**, 5367 (1999).
[4] C. H. Ho, P. C. Yen, Y. S. Huang, and K. K. Tiong, Phys. Rev. B **66**, 245207 (2002).
[5] C. H. Ho and C. E. Huang, J. Alloys Compd. **383**, 74 (2004).
[6] C. H. Ho, H. W. Lee, and C. C. Wu, J. Phys.: Condens. Matter **16**, 5937 (2004).
[7] K. F. Mak, C. Lee, J. Hone, J. Shan, and T. F. Heinz, Phys. Rev. Lett. **105**, 136805 (2010).
[8] A. Splendiani, L. Sun, Y. Zhang, T. Li, J. Kim, C.-Y. Chim, G. Galli, and F. Wang, Nano Lett. **10**, 1271 (2010).
[9] X. Xu, W. Yao, D. Xiao, and T. F. Heinz, Nat. Phys. **10**, 343 (2014).
[10] Z. Ye, T. Cao, K. O'Brien, H. Zhu, X. Yin, Y. Wang, S. G. Louie, and X. Zhang, Nature (London) **513**, 214 (2014).
[11] G. Wang, X. Marie, I. Gerber, T. Amand, D. Lagarde, L. Bouet, M. Vidal, A. Balocchi, and B. Urbaszek, Phys. Rev. Lett. **114**, 097403 (2015).
[12] S. Tongay, H. Sahin, C. Ko, A. Luce, W. Fan, K. Liu, J. Zhou, Y.-S. Huang, C.-H. Ho, J. Yan, D. F. Ogletree, S. Aloni, J. Ji, S. Li, J. Li, F. M. Peeters, and J. Wu, Nat. Commun. **5**, 1 (2014).
[13] S. Yang, S. Tongay, Y. Li, Q. Yue, J.-B. Xia, S.-S. Li, J. Li, and S.-H. Wei, Nanoscale **6**, 7226 (2014).
[14] D. Wolverson, S. Crampin, A. S. Kazemi, A. Ilie, and S. J. Bending, ACS Nano **8**, 11154 (2014).
[15] O. B. Aslan, D. A. Chenet, A. M. van der Zande, J. C. Hone, and T. F. Heinz, ACS Photon. **3**, 96 (2016).
[16] M. Rahman, K. Davey, and S.-Z. Qiao, Adv. Funct. Mater. **27**, 1606129 (2017).
[17] B. Jariwala, D. Voiry, A. Jindal, B. A. Chalke, R. Bapat, A. Thamizhavel, M. Chhowalla, M. Deshmukh, and A. Bhattacharya, Chem. Mater. **28**, 3352 (2016).
[18] M. Gehlmann, I. Aguilera, G. Bihlmayer, S. Nemšák, P. Nagler, P. Gospodarič, G. Zamborlini, M. Eschbach, V. Feyer, F. Kronast, E. Młyńczak, T. Korn, L. Plucinski, C. Schüller, S. Blügel, and C. M. Schneider, Nano Lett. **17**, 5187 (2017).
[19] I. Gutiérrez-Lezama, B. A. Reddy, N. Ubrig, and A. F. Morpurgo, 2D Materials **3**, 045016 (2016).
[20] J. L. Webb, L. S. Hart, D. Wolverson, C. Chen, J. Avila, and M. C. Asensio, Phys. Rev. B **96**, 115205 (2017).
[21] C. M. Fang, G. A. Wiegers, C. Haas, and R. A. d. Groot, J. Phys.: Condens. Matter **9**, 4411 (1997).
[22] H.-X. Zhong, S. Gao, J.-J. Shi, and L. Yang, Phys. Rev. B **92**, 115438 (2015).
[23] X. Zhang and Q. Li, J. Appl. Phys. **118**, 064306 (2015).
[24] E. Liu, Y. Fu, Y. Wang, Y. Feng, H. Liu, X. Wan, W. Zhou, B. Wang, L. Shao, C.-H. Ho, Y.-S. Huang, Z. Cao, L. Wang, A. Li, J. Zeng, F. Song, X. Wang, Y. Shi, H. Yuan, H. Y. Hwang, Y. Cui, F. Miao, and D. Xing, Nat. Commun. **6**, 6991 (2015).
[25] A. Arora, J. Noky, M. Drüppel, B. Jariwala, T. Deilmann, R. Schneider, R. Schmidt, O. Del Pozo-Zamudio, T. Stiehm, A. Bhattacharya, P. Krüger, S. Michaelis de Vasconcellos, M. Rohlfing, and R. Bratschitsch, Nano Lett. **17**, 3202 (2017).
[26] G. Wang, I. C. Gerber, L. Bouet, D. Lagarde, A. Balocchi, M. Vidal, T. Amand, X. Marie, and B. Urbaszek, 2D Mater. **2**, 1 (2015).
[27] K. Friemelt, M. C. Lux Steiner, and E. Bucher, J. Appl. Phys. **74**, 5266 (1993).
[28] K. Friemelt, L. Kulikova, L. Kulyuk, A. Siminel, E. Arushanov, C. Kloc, and E. Bucher, J. Appl. Phys. **79**, 9268 (1996).

[29] C. H. Ho, Y. S. Huang, and K. K. Tiong, J. Alloys Compd. **317-318**, 222 (2001).
[30] C. H. Ho, P. C. Yen, Y. S. Huang, and K. K. Tiong, J. Phys.: Condens. Matter **13**, 8145 (2001).
[31] G. Kresse and J. Hafner, Phys. Rev. B **47**, 558(R) (1993).
[32] G. Kresse and J. Furthmüller, Phys. Rev. B **54**, 11169 (1996).
[33] J. P. Perdew, K. Burke, and M. Ernzerhof, Phys. Rev. Lett. **77**, 3865 (1996).
[34] P. E. Blöchl, Phys. Rev. B **50**, 17953 (1994).
[35] G. Kresse and D. Joubert, Phys. Rev. B **59**, 1758 (1999).
[36] M. Dion, H. Rydberg, E. Schröder, D. C. Langreth, and B. I. Lundqvist, Phys. Rev. Lett. **92**, 246401 (2004).
[37] G. Román-Pérez and J. M. Soler, Phys. Rev. Lett. **103**, 096102 (2009).
[38] J. Klimeš, D. R. Bowler, and A. Michaelides, Phys. Rev. B **83**, 195131 (2011).
[39] K. Lee, E. D. Murray, L. Kong, B. I. Lundqvist, and D. C. Langreth, Phys. Rev. B **82**, 081101(R) (2010).
[40] F. Hüser, T. Olsen, and K. S. Thygesen, Phys. Rev. B **88**, 245309 (2013).
[41] A. R. Klots, A. K. M. Newaz, B. Wang, D. Prasai, H. Krzyzanowska, J. Lin, D. Caudel, N. J. Ghimire, J. Yan, B. L. Ivanov, K. A. Velizhanin, A. Burger, D. G. Mandrus, N. H. Tolk, S. T. Pantelides, and K. I. Bolotin, Sci. Rep. **4**, 6608 (2014).
[42] A. Molina-Sánchez, D. Sangalli, K. Hummer, A. Marini, and L. Wirtz, Phys. Rev. B **88**, 045412 (2013).
[43] M. Shishkin and G. Kresse, Phys. Rev. B **74**, 035101 (2006).
[44] A. A. Mostofi, J. R. Yates, Y.-S. Lee, I. Souza, D. Vanderbilt, and N. Marzari, Comput. Phys. Commun. **178**, 685 (2008).
[45] W. Hanke and L. J. Sham, Phys. Rev. Lett. **43**, 387 (1979).
[46] M. Rohlfing and S. G. Louie, Phys. Rev. Lett. **81**, 2312 (1998).
[47] L. Yang, J. Deslippe, C.-H. Park, M. L. Cohen, and S. G. Louie, Phys. Rev. Lett. **103**, 186802 (2009).
[48] M. Bernardi, M. Palummo, and J. C. Grossman, Nano Lett. **13**, 3664 (2013).
[49] R. He, J.-A. Yan, Z. Yin, Z. Ye, G. Ye, J. Cheng, J. Li, and C. H. Lui, Nano Lett. **16**, 1404 (2016).
[50] Y.-C. Lin, H.-P. Komsa, C.-H. Yeh, T. Björkman, Z.-Y. Liang, C.-H. Ho, Y.-S. Huang, P.-W. Chiu, A. V. Krasheninnikov, and K. Suenaga, ACS Nano **9**, 11249 (2015).
[51] H. H. Murray, S. P. Kelty, R. R. Chianelli, and C. S. Day, Inorg. Chem. **33**, 4418 (1994).
[52] J. C. Wildervanck and F. Jellinek, J. Less Common Metals **24**, 73 (1971).
[53] J. He, K. Hummer, and C. Franchini, Phys. Rev. B **89**, 075409 (2014).
[54] J. P. Echeverry, B. Urbaszek, T. Amand, X. Marie, and I. C. Gerber, Phys. Rev. B **93**, 121107(R) (2016).
[55] C. Robert, T. Amand, F. Cadiz, D. Lagarde, E. Courtade, M. Manca, T. Taniguchi, K. Watanabe, B. Urbaszek, and X. Marie, Phys. Rev. B **96**, 155423 (2017).
[56] J. V. Marzik, R. Kershaw, K. Dwight, and A. Wold, J. Solid State Chem. **51**, 170 (1984).
[57] B. L. Wheeler, J. K. Leland, and A. J. Bard, J. Electrochem. Soc. **133**, 358 (1986).
[58] H. Zhao, J. Wu, H. Zhong, Q. Guo, X. Wang, F. Xia, L. Yang, P. Tan, and H. Wang, Nano Res. **8**, 3651 (2015).
[59] A. Tkatchenko and M. Scheffler, Phys. Rev. Lett. **102**, 073005 (2009).
[60] S. Grimme, J. Antony, S. Ehrlich, and H. Krieg, J. Chem. Phys. **132**, 154104 (2010).